Journal of Solid State Chemistry **145,** 573–579 (1999)
Article ID jssc.1999.8225, available online at http://www.idealibrary.com on IDEAL®

The Structure of Amorphous CrS_3 Containing $[Cr^{III}_2((S^{-I})_2)_3]_x$ Chains: An X-Ray Diffraction Modeling Study

Simon J. Hibble,*,[1] Richard I. Walton,* Alex C. Hannon,† and Graham Bushnell-Wye‡

*Department of Chemistry, University of Reading, Whiteknights, PO Box 224, Reading, RG6 6AD, United Kingdom; †ISIS Facility, Rutherford Appleton Laboratory, Chilton, Didcot, Oxon, OX11 0QX, United Kingdom; and ‡CLRC Daresbury Laboratory, Warrington, Cheshire, WA4 4AD, United Kingdom

Received October 30, 1998; in revised form February 12, 1999; accepted February 13, 1999

The amorphous chromium sulfide, CrS_3, has no crystalline counterpart. A model is constructed to account for the interference function, $Qi(Q)$, and the real space total correlation function, $T(r)$, obtained from X-ray diffraction measurements. The structural unit $(S^{-I})_{2/2}Cr^{III}((S^{-I})_2))_2Cr^{III}(S^{-I})_{2/2}$ gives a good fit to the Q-space data over the range 2–20 Å^{-1} and explains features in $T(r)$ to 3.6 Å. The unprecedented coordination geometry around chromium explains the unusual magnetic moment of the compound, corresponding to one unpaired electron per Cr^{III}. The individual structural units are linked by the terminal disulfide groups to give $[-Cr(S_2)_2Cr(S_2)-]_n$ chains. The flexibility of the single disulfide linkages within the chains and the difficulty of rearranging these chains to form an ordered structure after the rapid formation of CrS_3 from solution explains the amorphous nature of CrS_3. © 1999 Academic Press

INTRODUCTION

Amorphous transition-metal sulfides have attracted much attention because they possess a wide variety of chemical and physical properties. Of particular interest are materials which have sulfur-to-metal ratios different to those found for the crystalline sulfides of the corresponding metal, such as MoS_3, Re_2S_7, and V_2S_5; these compounds have been shown to possess interesting electrochemical and catalytic properties (1–3). We recently prepared a new amorphous chromium sulfide, a-CrS_3, using a novel low-temperature ($< 200°C$) method (4). This compound is of significant interest because it is the most sulfur-rich sulfide of chromium and also because it has no crystalline counterpart.

A number of early transition metals form crystalline sulfides with high sulfur-to-metal content and we viewed these compounds as possible structural models for a-CrS_3. The trisulfides of Ti, Zr, Hf, Nb, and Ta are best formulated as $M^{IV}S^{2-}(S_2)^{2-}$. All adopt closely related structures in which closely packed chains are found. In each case, the metal is found in approximate trigonal-prismatic coordination, with distortions introduced by sulfur–sulfur bonding between 2/3 of the sulfur atoms, which form $(S_2)^{2-}$ groups (5). The vanadium sulfide, VS_4, is the most sulfur-rich crystalline transition-metal sulfide (6). In this compound all the sulfur atoms are found in disulfide groups and the compound is formulated as $V^{IV}(S_2{}^{2-})_2$. Pairs of disulfide anions bridge pairs of vanadium atoms to form infinite chains with vanadium adopting eight-fold coordination. The chains are held together only by van der Waal interactions. These sulfur-rich crystalline transition-metal sulfides all exhibit two important features: they have one-dimensional structures and all contain appreciable sulfur–sulfur bonding.

In our X-ray absorption fine structure (EXAFS) study (7) of a-CrS_3 we found that each chromium was surrounded by six sulfur atoms, at 2.35 Å, and that each sulfur was bound to two chromiums and also to one sulfur, at 2.03 Å, to form disulfide groups. Close examination of the near-edge structure of the sulfur K-edge and comparison with data from model compounds confirmed that sulfur is located exclusively in disulfide anions, and this was further supported by infrared spectroscopy results. We thus formulated the material as $Cr^{III}(S_2^{2-})_{1.5}$ and proposed two possible structures for this material based on $CrS_{6/2}$ units. Figure 1 shows the constituent units of the two structures. The units in Fig. 1a can be linked to form individual chains and those in Fig. 1b can be linked to form chains joined by bridging disulfides. Since no information about interatomic distances beyond ~ 2.5 Å was obtained in the EXAFS study, no definitive conclusion about the coordination geometry around $CrS_{6/2}$ units or their mode of linkage could be reached, and we were unable to decide which of the proposed structures was correct. To test the validity of the two structures we needed information on longer interatomic correlations than we could obtain in the EXAFS study. Such information can be obtained from diffraction data, which yield data down to

[1]To whom correspondence should be addressed.

0022-4596/99 $30.00

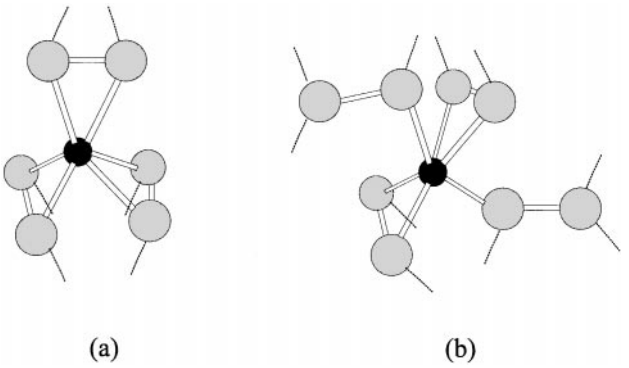

FIG. 1. Two possible structural units which might make up the structure of amorphous CrS_3 based on EXAFS results. Small filled circles, chromium; large shaded circles, sulfur. Broken lines represent S–Cr bonds to other similar units.

shorter distances in reciprocal space (small Q). This is impossible in an EXAFS experiment because of the presence of multiple scattering in the low k-region. Such data are essential in determining medium range order in amorphous compounds, because disorder means that longer range correlations make only a very small contribution at high Q. Other factors such as photoelectron lifetime also reduce the magnitude of the EXAFS signal arising from longer range correlations. An additional advantage of diffraction data collected to low Q is that this enables a more accurate determination of coordination numbers than is possible using EXAFS. We therefore turned to X-ray diffraction to gain a fuller understanding of the structure of a-CrS_3.

Information on atomic correlations contained in the interference function $Qi(Q)$, obtained from a diffraction experiment is most easily visualized by Fourier transformation to yield a real-space correlation function (8). Interpretation of this function is, however, not straightforward because of appreciable peak overlap at all but the smallest distances. In this work we have carried out comparisons in both reciprocal and real space. We compare both $Qi(Q)$ and the total correlation function $T(r)$ calculated from our model with those determined experimentally.

EXPERIMENTAL

A sample of a-CrS_3 was prepared by reaction between $Cr(CO)_6$ and elemental sulfur in boiling 1,2-dichlorobenzene, in the molar ratio 1:7, as described in our previous work (7). The mixture was heated for 2 hours after dry nitrogen gas had been bubbled through for 30 minutes. A black precipitate of a-CrS_3 was seen to form within the first 5 minutes of heating. The solid was thoroughly washed with carbon disulfide to remove unreacted sulfur and dried under vacuum. The pycnometric density of the material was determined as 3.1(1) gcm^{-3} by liquid displacement. X-ray diffraction data were collected from a sample of the material of around 0.375-mm thickness in a Kapton sample holder of dimensions 10×30 mm on Station 9.1 of the Daresbury SRS (9). Data were collected using a symmetrical θ–2θ transmission technique in steps less than the equivalent of $\Delta Q = 0.05$ Å^{-1}, interpolated to produce data with constant Q steps of this size over the Q range 0.4–22.4 Å^{-1}, and extrapolated to $Q = 0$ Å^{-1}. The diffracted intensity was measured using the Warren–Mavel technique (10) to minimize Compton scattering. The incident X-ray wavelength was set at a value slightly higher than the Ag$K\alpha$ edge (0.4875 Å) using a Si[1 1 1] monochromator, and the diffracted X-rays were detected by observing the fluorescence excited in a thin (~ 30 μm) silver foil.

DATA REDUCTION AND RESULTS

Standard procedures were used to correct the diffraction data for experimental factors (absorption, polarization effects, etc) and the high-angle method used for normalization, to yield the sharpened distinct scattering $i(Q)$ for CrS_3 (8).

$$i(\mathrm{Q}) = (c_{\mathrm{Cr}}Z_{\mathrm{Cr}} + c_{\mathrm{S}}Z_{\mathrm{S}})^2\,((I_{eu}/N(c_{\mathrm{Cr}}f_{\mathrm{Cr}}(Q) + c_{\mathrm{S}}f_{\mathrm{S}}(Q))^2) - 1) \quad [1]$$

I_{eu} is the scattering from the CrS_3 sample in electron units after correction for experimental factors, c_{Cr} and c_{S} are the atomic fractions of chromium and sulfur, respectively, Z_{Cr} and Z_{S} the corresponding atomic numbers, and f_{Cr} and f_{S} the X-ray form factors for chromium and sulfur; N is the number of atoms in the sample. Figure 2 shows the distinct scattering over the range 0–20 Å^{-1} and Fig. 3 the interference function, $Qi(Q)$. The sharp first peak observed in the diffraction data at low Q (at $Q = 1.00$ Å^{-1}) in $i(Q)$) is a feature commonly observed for amorphous or poorly crystalline materials and is associated with medium range order in the material (11).

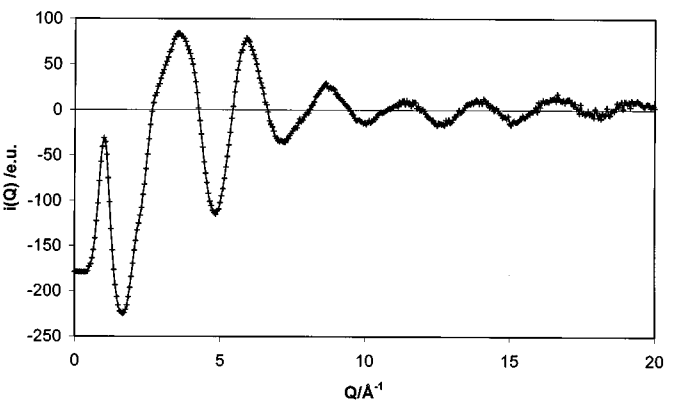

FIG. 2. The distinct scattering, $i(Q)$, for amorphous CrS_3; data points (crosses) are joined by a line to aid the eye.

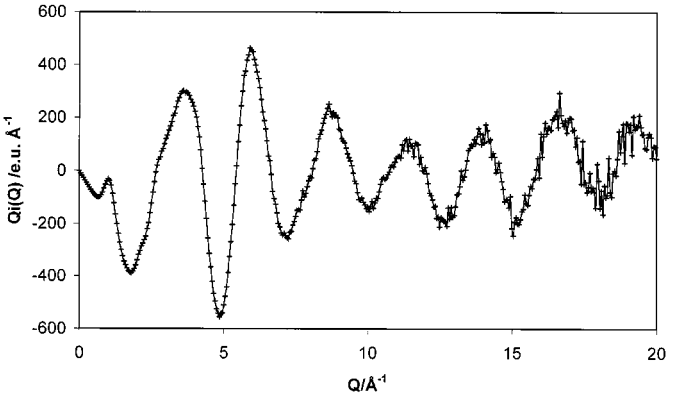

FIG. 3. The interference function, $Qi(Q)$, for amorphous CrS_3; data points (crosses) are joined by a line to aid the eye.

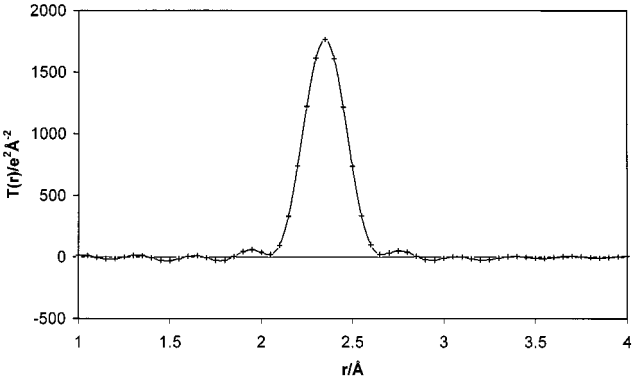

FIG. 5. $T(r)$ calculated for a single Cr–S correlation at 2.35 Å, showing the magnitude of termination ripples produced by the finite data range of $Qi(Q)$.

The $Qi(Q)$ data were Fourier transformed to yield the differential correlation function,

$$D(r) = \frac{2}{\pi}\int_0^{Q_{max}} Qi(Q)\sin(rQ)\,dQ, \qquad [2]$$

where Q_{max} is the maximum value of Q for the data. This was converted to the total correlation function,

$$T(r) = D(r) + 4\pi r\rho_0(c_{Cr}Z_{Cr} + c_SZ_S)^2, \qquad [3]$$

where ρ_0 is the measured bulk atomic number density. Figure 4 shows the total correlation function, $T(r)$, for a-CrS_3. It should be noted that we have not adopted the usual practice and employed a modification function to minimize termination ripples arising from the data being collected to a finite Q_{max}, preferring to retain the maximum resolution in $T(r)$. Figure 5 shows that the magnitude of the termination ripples arising from the principal peak centered at 2.35 Å is much lower than the features of interest in $T(r)$.

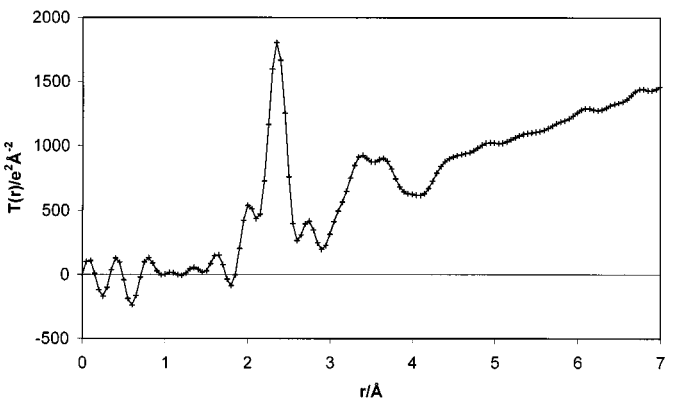

FIG. 4. The total correlation function, $T(r)$, for amorphous CrS_3; calculated points (crosses) are joined by a line to aid the eye.

It is important to note that the termination ripples present in the experimental $T(r)$ are also included in our model.

The first two peaks in $T(r)$, Fig. 4, centered at 2.02 and 2.35 Å contain information about the S–S correlations of disulfide groups and Cr–S bonded distances, respectively. The values found are in good agreement with the S–S distance of 2.03 ± 0.09 Å and the Cr–S bonded distance of 2.351 ± 0.002 Å determined in the previous EXAFS study (5). No information on correlations at larger distances was obtained from EXAFS studies. It can immediately be seen from Fig. 4 that X-ray diffraction yields information on correlations to higher r than the EXAFS study. The correlation function $T(r)$ contains information about nonbonded correlations which is vital to the determination of the geometry of the CrS_6 units and their mode of connection.

MODELING

The Debye equation (11) was used to calculate $i(Q)_{calc}$, and hence $Qi(Q)_{calc}$ for the models

$$i(Q)_{calc} = \left(\sum_m \sum_{n\neq m} f(Q)_m f(Q)_n \frac{\sin Qr_{mn}}{Qr_{mn}} \exp\left(\frac{-\langle u_{mn}^2\rangle Q^2}{2}\right)\right) \times (c_{Cr}Z_{Cr} + c_SZ_S)^2/4(c_{Cr}f_{Cr}(Q) + c_Sf_S(Q))^2, \qquad [4]$$

where $f_m(Q)$ and $f_n(Q)$ are the form factors of the atoms m and n, r_{mn} is the interatomic distance of a given atom pair, $\langle u_{mn}^2\rangle$ is the mean square variation in distance, and the sum is over the atoms in a CrS_3 unit. Division by four gives $i(Q)$ for an average atom. Form-factors were calculated using the analytical approximation (12).

The "goodness of fit" between Q-space data calculated for various models and the experimental data have been

reported in terms of an R_Q-factor,

$$R_Q = \sqrt{\frac{\sum_{i=Q_{\min}}^{i=Q_{\max}} (\mathrm{obs}_i - \mathrm{calc}_i)^2}{\sum_{i=Q_{\min}}^{i=Q_{\max}} \mathrm{obs}_i^2}}, \quad [5]$$

where obs_i and calc_i are the ith experimental and calculated data points for the experimental and theoretical $Qi(Q)$, respectively. The goodness of fit between $T(r)$ calculated for various models and the experimental data have been reported in terms of an $R_{T(r)}$-factor,

$$R_{T(r)} = \sqrt{\frac{\sum_{i=r_{\min}}^{i=r_{\max}} (\exp_i - \mathrm{calc}_i)^2}{\sum_{i=r_{\min}}^{i=r_{\max}} \exp_i{}^2}}, \quad [6]$$

where $\exp_i$ and calc_i are the ith data points for the experimentally determined and calculated $T(r)$, respectively.

We concentrated on modeling the short and medium range order in an attempt to determine the basic structural unit in a a-CrS_3, and therefore modeled the $Qi(Q)$ data over the Q-range 2–20 $Å^{-1}$. Using the average Cr–S and S–S distances and coordination numbers derived from our EXAFS study (5) and the $\langle u_{mn}^2 \rangle$ values given in Table 1 we could account for the majority of the structure in $Qi(Q)$ ($R_Q = 0.490$); see Fig. 6a. This simple model, Model 1, also gave an excellent fit to the first two peaks in $T(r)$ ($R_{T(r)} = 0.088$ over the r range 1.5–2.6 Å); see Fig. 7a. This demonstrates that the material does indeed contain 6-coordinate chromium and exclusively disulfide groups and that the coordination numbers found in our EXAFS study (7) were correct.

TABLE 1
Model Parameters for a-CrS_3 Models 1, 2, and 3

	Model parameters			
Pair	Distance/Å	Number of correlations per CrS_3 unit	$\langle u^2 \rangle$/Å^2	Included in
Cr–S and S–Cr	2·35	12	0.012	Models 1, 2, and 3
S–S	2.02	3	0.0014	Models 1, 2, and 3
S ⋯ S	2.73	2	0.006	Models 2 and 3
S ⋯ S	3.39	2	0.006	Models 2 and 3
Cr ⋯ Cr	3.25	1	0.006	Models 2 and 3
Cr ⋯ Cr	3.60	1	0.008	Model 3

Note. Model 1: $R_Q = 0.490$. $R_{T(r)} = 0.088$ over the r range 1.5–2.6 Å. $R_{T(r)} = 0.229$ over the r range 1.5–3.0 Å. $R_{T(r)} = 0.689$ over the r range 1.5–4.0 Å. Model 2: $R_Q = 0.415$. $R_{T(r)} = 0.077$ over the r range 1.5–2.6 Å. $R_{T(r)} = 0.162$ over the r range 1.5–3.0 Å. $R_{T(r)} = 0.609$ over the r range 1.5–4.0 Å. Model 3: $R_Q = 0.364$. $R_{T(r)} = 0.077$ over the r range 1.5–2.6 Å. $R_{T(r)} = 0.165$ over the r range 1.5–3.0 Å. $R_{T(r)} = 0.567$ over the r range 1.5–4.0 Å.

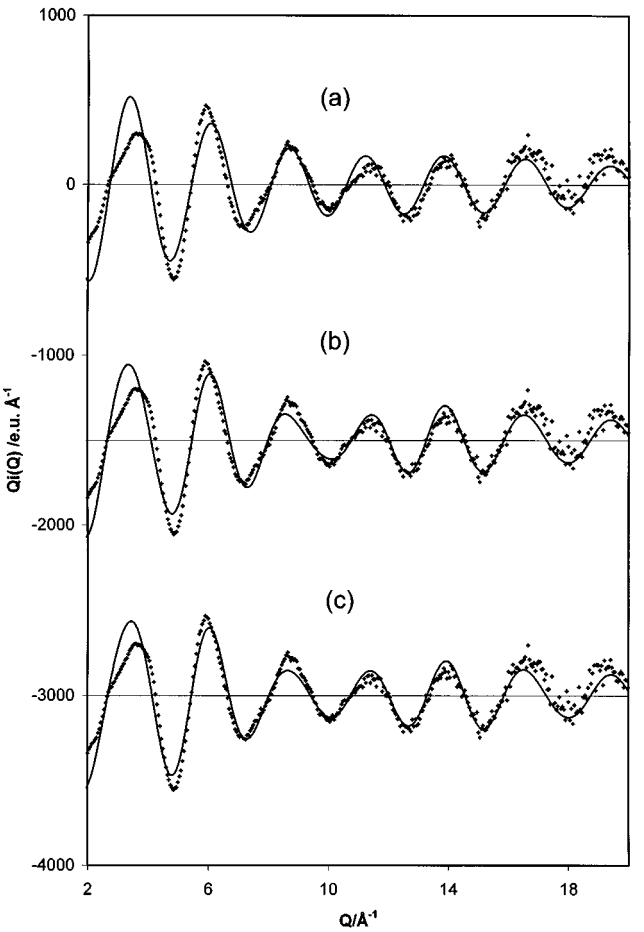

FIG. 6. (a) The interference function, $Qi(Q)$ for a-CrS_3 (crosses) and $Qi(Q)_{\mathrm{calc}}$ (solid line) generated by Model 1. (b) $Qi(Q)$ for a-CrS_3 (crosses) and $Qi(Q)_{\mathrm{calc}}$ (solid line) generated by Model 2 offset by -1500. (c) $Qi(Q)$ for a-CrS_3 (crosses) and $Qi(Q)_{\mathrm{calc}}$ (solid line) generated by Model 3 offset by -3000.

We now had to consider how the CrS_6 units were linked together and the resulting geometry of the CrS_6 unit. The feature occurring at 2.73 Å in $T(r)$ provides the key. There is no evidence for a correlation at this distance in the chromium k-edge EXAFS (7). The k-range and hence resolution of those data was sufficient to resolve a Cr–S or Cr–Cr correlation at that distance if it were present in a-CrS_3. Hence, we ascribe this correlation to nonbonded S ⋯ S correlations. There does indeed appear to be a feature in the Fourier transform of the S K-edge EXAFS data beyond the broad peak due to bonded S–S and S–Cr correlations, but this is not resolved due to the shorter k-range of this data. A short S ⋯ S correlation is a natural consequence of connecting the units shown in Fig. 1a to form chains, and as we will show it was possible to construct a chemically and physically reasonable model, which is compatible with our X-ray diffraction measurements and the derived $T(r)$. This

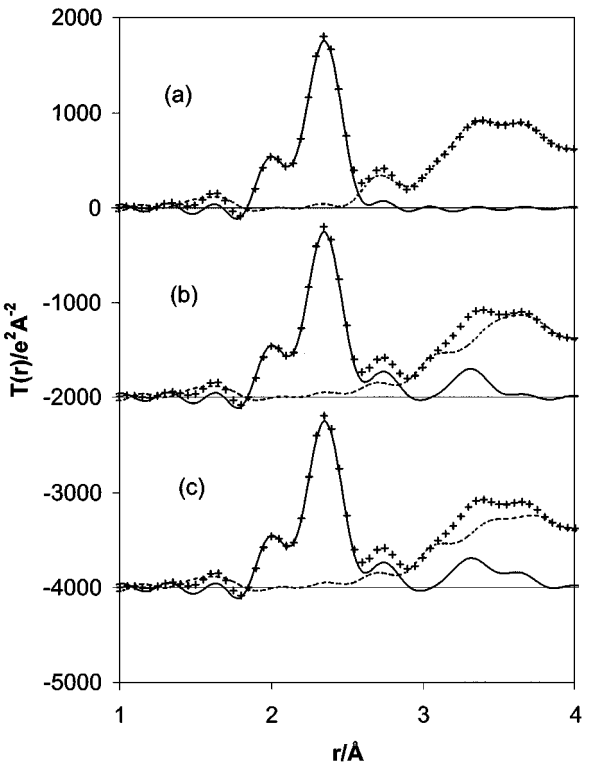

FIG. 7. (a) $T(r)$ (crosses) for a-CrS_3, $T(r)_{calc}$ (solid line) and $T(r)_{residual}$ (broken line) generated by Model 1. (b) $T(r)$ for a-CrS_3, $T(r)_{calc}$ (solid line) and $T(r)_{residual}$ (broken line) generated by Model 2 offset by -2000. (c) $T(r)$ for a-CrS_3, $T(r)_{calc}$ (solid line) and $T(r)_{residual}$ (broken line) generated by Model 3 offset by -4000.

was not possible using the units shown in Fig. 1b. We used the V–$\{(S_2^{2-})_2\}$–V linkage found in crystalline VS_4 (6) as a model to produce the Cr_2S_8 structural unit shown in Fig. 8. This figure also shows how the unit is linked to similar units via disulfide bridges to chromium atoms in adjacent units. In this way chains, $[-Cr(S_2)_2Cr(S_2)-]_n$, are produced and for large n the composition approaches CrS_3.

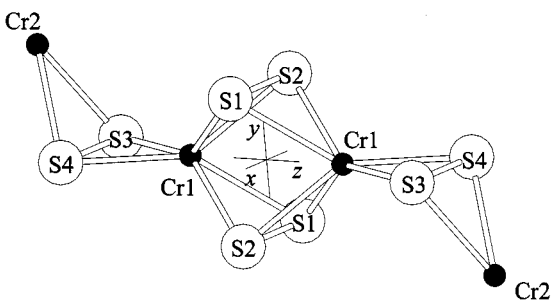

FIG. 8. The Cr_2S_8 structural building block and chromium atoms in neighboring units used to model the diffraction data from a-CrS_3. The atomic numbering scheme and axes correspond to those used in Table 2.

We fixed the Cr–S and S–S distances at the values found above and added the contribution due to Cr ··· Cr and S ··· S correlations in the rigid central portion of the Cr_2S_8 unit to our calculation of $Qi(Q)$ and $T(r)$. We now varied Cr ··· Cr to give the best fit to $Qi(Q)$ and $T(r)$. The minimum R-factors occurred when Cr ··· Cr equalled 3.25 Å, producing a short nonbonded S ··· S distance of 2.73 Å (e.g., S1 ··· S2) and a long nonbonded S ··· S (e.g., S1 ··· S1) distance of 3.39 Å. This is Model 2, and the fits to $Qi(Q)$ and $T(r)$, are shown in Figs. 6b and 7b, respectively. This model accounts for the peak in $T(r)$ at 2.73 Å and some of the structure at around 3.3 Å in $T(r)$. It is not surprising that the nonbonded Cr1 ··· Cr1 distance of 3.25 Å is not seen in the EXAFS study, since even in crystalline VS_4 the nonbonded V ··· V distance of 3.2 Å is hardly visible in the EXAFS work. The short S ··· S distance in the central unit is a consequence of the Cr–S bond distance combined with the geometrical constraint of the double disulfide link and the repulsion of the nonbonded Cr^{III} atoms. The nonbonded correlations involving the remaining disulfide group S(3)–S(4) are more difficult to model because of the lack of sharp features in $T(r)$. This is characteristic of amorphous materials, where there is by definition disorder at longer length scales. Clearly we need to explain how this disorder arises in our model. The constraints on the remaining disulfide groups are much less severe than on those in the double disulfide bridge. These disulfide groups, which are involved in Cr–(S_2^{2-})–Cr linkages to other Cr_2S_8 units to produce $[-Cr(S_2)_2Cr(S_2)-]_n$ chains, can rotate, and the chain can flex around them to produce the type of disordered structure, shown in Fig. 9. Correlations involving the sulfides in the Cr–(S_2^{2-})–Cr linkages would therefore not be expected to

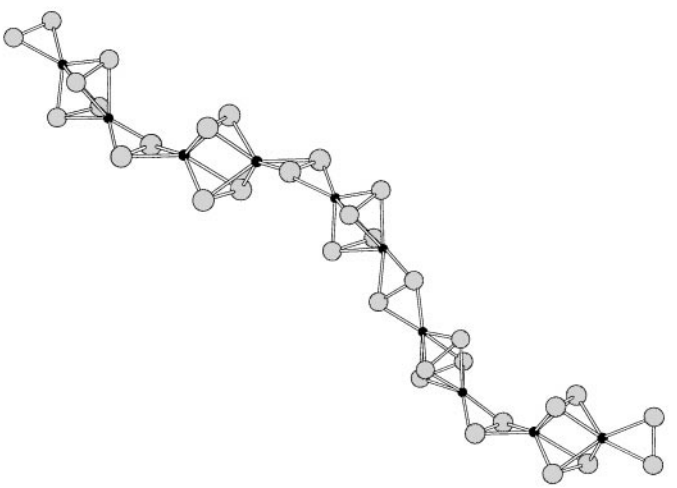

FIG. 9. A schematic of a disordered CrS_3 chain showing how disorder might arise from the flexible linkages between the $(S^{-1})_{2/2}Cr^{III}((S^{-1})_2))_2$ $Cr^{III}(S^{-1})_{2/2}$ structural units. Small filled circles, chromium; large shaded circles, sulfur.

TABLE 2
Atomic Coordinates of the Cr_2S_8 Unit Used to Model the X-Ray Diffraction Data (Atoms at x, y, z and $-x, -y, -z$)[a]

Atom	Coordinates (x, y, z)
S1	(1.01, 1.364, 0.0)
S2	(−1.01, 1.364, 0.0)
S3	(−1.01, 0.0, 3.747)
S4	(−1.01, 0.0, 3.747)
Cr1	(0.0000, 0.0000, 1.625)
Cr2	(0.0000, 1.902, 4.682)

[a]See Fig. 2 for definition of axes.

occur at well-defined distances and we have not included them in our modeling. Moreover, these correlations will occur beyond the range of the well-defined structure in $T(r)$ and overlap with interchain S–S correlations.

In our final model, Model 3, we have included a contribution from Cr1 ⋯ Cr2 correlations arising from linking Cr_2S_8 units together; see Table 1. A value of 3.60 Å gives a Cr–S–Cr bond angle of 100°. Flexing of the chain would be expected to produce a range of bond angles around the average value and this is reflected in the high mean-squared variation in the Cr–Cr distance. Including this correlation we got a marked improvement in the fit to $Qi(Q)$, see Fig. 6c, and a final fit index $R_Q = 0.364$. This Cr ⋯ Cr correlation accounts for the structure seen in $T(r)$ at about 3.6 Å; see Fig. 7c. However, it should be noted that the total correlation function at this distance will have a large number of other contributions from both intra- and interchain correlations. Atomic coordinates for the final model are given in Table 2.

As a final check on the validity of our model we ignored the EXAFS evidence on the structure of CrS_3 and attempted to produce other models to account for the correlation seen in $T(r)$ at 2.73 Å. Ascribing this to a Cr–S correlation always produced unreasonable S–S contacts, lying in the troughs of $T(r)$, which put surprisingly large constraints on producing a simple model. We could produce no satisfactory model to account for the $Qi(Q)$ data and $T(r)$ based on the assumption that this feature in $T(r)$ arose from a Cr–S correlation. Ascribing the feature in $T(r)$ at 2.73 Å to a Cr–Cr bond produced, in addition to chemically unreasonable models, much higher R-factors for the fit to $Qi(Q)$.

DISCUSSION

Our model has successfully accounted for the structure in $Qi(Q)$ and accounts for the features seen in $T(r)$. We therefore believe it comes close to portraying the true structure of a-CrS_3. The short nonbonded S ⋯ S distances in the Cr_2S_8 structural unit are a little shorter, but comparable to those found in related crystalline metal sulfides with $M(S_2)_2M$ linkages, for example in VS_4 ($V^{IV}(S_2^{2-})_2$) S ⋯ S = 2.98 Å (6) and in TiS_3 ($Ti^{IV}(S^{2-})(S_2^{2-})$) S ⋯ S = 2.92 Å (5). We note that the volume per sulfur atom in CrS_3 of 26.5 Å^3 is very close to that found in crystalline VS_4 in which the corresponding value is 26.3 Å^3. This provides further evidence that CrS_3 contains all the sulfur atoms in S_2^{2-} groups and that it, like VS_4, adopts a chain structure. We envisage a-CrS_3 to consist of a tangle of chains of the type shown in Fig. 9.

An important point that has emerged from the modeling study is that the local coordination geometry around chromium is highly distorted from the almost regular octahedral geometry normally found for the Cr^{III} d^3 ion. The most unusual geometry for the Cr^{III} d^3 ion, with C_{2v} symmetry in our model, must explain the very unusual magnetic susceptibility of CrS_3, which gave an unprecedented value of $\mu = 1.73$ B.M. suggesting only one unpaired electron per Cr^{III} (7).

Although we have accounted for the principal features in $T(r)$, we have not accurately modeled $T(r)$ about 3 Å. This is because interchain nonbonded correlations make a large contribution beyond this distance. We have not built a large enough model to include these correlations and with the limited information in $T(r)$; we do not believe this can be done reliably. Omitting such correlations also affects the peak in $T(r)$ at 2.73 Å since the tail of the contribution from longer S ⋯ S will lift this peak closer to the experimental values.

CONCLUSIONS

The fit to the experimental data of our final structural model of a-CrS_3 is very good both in Q-space and in r-space. A simple structural unit containing 12 atoms can account for most of the structure seen in $Qi(Q)$. The central part of this unit, $Cr(S_2)_2Cr$, appears to be rigid but the linkage to similar units via bridging disulfides to form infinite chains, $Cr(S_2)[Cr(S_2)_2Cr(S_2)]_\infty Cr$, is relatively flexible. This explains why the material is amorphous.

ACKNOWLEDGMENTS

We thank the EPSRC for provision of a studentship (RIW) and synchrotron X-ray facilities at Daresbury Laboratory.

REFERENCES

1. R. R. Chianelli, *Int. Rev. Phys. Chem.* **2,** 127 (1982).
2. T. Weber, J. C. Muijsers, and J. W. Niemantsverdriet, *J. Phys. Chem.* **99,** 9194 (1995).
3. A. Müller, E. Krickemeyer, H. Bögge, H. Ratajczak, and A. Armatage, *Angew. Chem. Int. Ed. Eng.* **33,** 272 (1994).
4. S. J. Hibble, D. A. Rice, M. J. Almond, K. A. Hassan Mohammad, S. P. Pearse, and J. R. Sagar, *J. Mater. Chem.* **2,** 1237 (1992).

5. S. K. Srivastava and B. N. Avasthi, *J. Mater. Sci.* **27,** 3693 (1992).
6. R. Allmann, I. Baumann, A. Kutoglu, H. Rösch, and E. Hellner, *Naturwissenschaften* **51,** 263 (1964).
7. S. J. Hibble. R. I. Walton, and D. M. Pickup, *J. Chem. Soc., Dalton Trans.* 2245 (1996).
8. B. E. Warren, "X-Ray Diffraction," Chap. 10. Dover, New York, 1990.
9. G. Busnell-Wye and R. J. Cernik, *Rev. Sci. Instrum.* **63,** 999 (1992).
10. B. E. Warren and G. Mavel, *Rev. Sci. Instrum.* **36,** 196 (1965).
11. S. R. Elliot, "Physics of Amorphous Materials," 2nd. ed. Longman, Harlow/Essex, 1990.
12. E. N. Maslen, A. G. Fox, and M. A. O'Keefe, *in* "International Tables for Crystallography," Vol. C, p. 487. Kluwer, Dordrect, 1995.